THE
PHYSICAL REVIEW

A journal of experimental and theoretical physics established by E. L. Nichols in 1893

SECOND SERIES, VOL. 160, NO. 4 20 AUGUST 1967

Solution of Coupled Equations by *R*-Matrix Techniques*

P. J. A. BUTTLE†
Department of Physics, Florida State University, Tallahassee, Florida
(Received 10 February 1967)

A realistic coupled-equation problem is solved using various *R*-matrix and level-matrix techniques. Comparison with exact coupled-equation calculations shows that excellent numerical results are possible with these methods, both in resonant and in nonresonant energy regions. The effects of varying the *R*-matrix boundary conditions and the number of levels included in the calculation are considered. Various aspects of *R*-matrix theory, such as the composition of *R*-matrix states, and the interference between neighboring levels, are illustrated by the calculations.

I. INTRODUCTION

A VARIETY of formal theories of nuclear reactions have been proposed in the last 30 years. A discussion of these and a list of references may be found in a recent paper by Lane and Robson,[1] in which a comprehensive formalism covering many of the earlier theories is suggested. Such formal theories have been of great value in providing a theoretical understanding of nuclear reactions, and in suggesting algebraic forms which experimental data should follow and parameters by which they may be characterized. Except for the simple potential-scattering problem however, little work of a numerical nature has been done in the way of starting with a Hamiltonian and using it to calculate resonance parameters and cross sections. Possible exceptions to this are the calculations based on Feshbach's[2] channel-coupling theory by Lemmer and Shakin,[3] and more recently by Lovas.[4] Reaction calculations have also been attempted recently by Tobocman *et al.*[5] starting with a shell-model Hamiltonian.

The coupled-equation theory suggested by the work of Feshbach, and which is used by various authors[6,7] in the analysis of scattering from collective nuclei, provides a suitable problem which we may attempt to solve in terms of the more formal theories. It is capable of exact solution by numerical methods,[6,7] and yet is less trivial than the one-channel potential-scattering problem, providing narrow resonances of the type observed in nuclear reactions. The purpose of this paper is to investigate the solution of this problem using *R*-matrix theory,[8] one of the better known of the formal theories. Haglund and Robson[9] have done calculations for a two-channel model using square-well potentials, and the results of their work indicate that only a few *R*-matrix levels need be included in the calculation. In this paper we consider a more realistic problem, that of a spin-$\frac{1}{2}$ projectile scattered by a 0^+-2^+ target, and compare our results with exact solutions obtained from the coupled-equation program written by Buck.[6] In solving the problem for a large number of incident energies, the *R*-matrix technique may also turn out to be more efficient than the conventional solution.

A further reason for doing calculations on the lines suggested by the formal reaction theories is that this may lead to a better understanding of the structure of resonances appearing in the scattering data. The work of Tobocman *et al.*,[5] and of Lemmer and Shakin[3] is

* Research supported in part by the U. S. Air Force Office of Scientific Research, Office of Aerospace Research, U. S. Air Force, under AFOSR Grant No. AFOSR-440-66 and the National Science Foundation under Grant No. NSF-GP-5114.

† Present address: University of Manchester, Manchester, England.

[1] A. M. Lane and D. Robson, Phys. Rev. **151**, 774 (1966).

[2] H. Feshbach, Ann. Phys. (N. Y.) **5**, 357 (1958); **19**, 287 (1962).

[3] R. Lemmer and C. M. Shakin, Ann. Phys. (N. Y.) **27**, 13 (1964).

[4] I. Lovas, Nucl. Phys. **81**, 353 (1966).

[5] W. Tobocman and M. A. Nagarajan, Phys. Rev. **138**, B1351 (1965); M. A. Nagarajan, S. K. Shah, and W. Tobocman, *ibid.* **140**, B63 (1965).

[6] B. Buck, Phys. Rev. **130**, 712 (1963).

[7] D. M. Chase, L. Wilets, and A. R. Edmonds, Phys. Rev. **110**, 1080 (1958).

[8] A. M. Lane and R. G. Thomas, Rev. Mod. Phys. **30**, 257 (1958).

[9] M. E. Haglund and D. Robson, Phys. Letters **14**, 225 (1965).

directed towards this end, and the calculations of Lovas[4] are an interesting application to the levels produced in the scattering of neutrons by C^{12}.

In Sec. II we indicate how the cross section may be expressed in the R-matrix formalism, and briefly state the coupled-equation problem which we are trying to solve. In Sec. III we introduce three methods of solution, the first two based on R-matrix theory and the third on the formalism derived by Sano, Yoshida, and Teresawa.[10] The results of calculations for both nonresonant and resonant energy regions are presented in Sec. IV, and the effect of varying the number of levels and boundary conditions is discussed. The calculations also demonstrate some of the effects of interference between neighboring R-matrix levels.

II. A BRIEF DERIVATION OF R-MATRIX THEORY AND STATEMENT OF THE COUPLED-EQUATION PROBLEM

R-matrix theory is adequately presented and discussed in the review article by Lane and Thomas.[8] For completeness, however, we will indicate how the cross section may be written in terms of the R matrix, and will use a slightly different viewpoint, starting with the transition amplitude T_{fi} between an initial state i and a final state f, which is more familiar to those working in the field of direct reactions.

Suppose that the target and projectile are described by spins I and s respectively, with z components K and σ, and that there are two final particles with spins $I'K'$ and $s'\sigma'$. Let $\mathbf{k}$ and $\mathbf{k}'$ be the initial and final relative wave vectors. Other quantum numbers will not be written down explicitly. The cross section for this process may be written[11]

$$\frac{d\sigma}{d\Omega}=\frac{mm'}{(2\pi\hbar^2)^2}\frac{k'}{k}|T_{fi}|^2, \tag{2.1}$$

where m, m' are the initial and final reduced masses, and

$$T_{fi}=\langle\chi_f^{(-)}|U_f|\phi_i\rangle+\langle\chi_f^{(-)}|(V_f-U_f)|\Psi_i^{(+)}\rangle. \tag{2.2}$$

$\Psi_i^{(+)}$ is the full solution corresponding to an incident plane wave $\phi_i=e^{i\mathbf{k}\cdot\mathbf{r}}|s\sigma\rangle|IK\rangle$, and $\chi_f^{(-)}$ is a final-state distorted wave calculated for an approximate final potential U_f. V_f is the actual final interaction. It is convenient to choose U_f to be the Coulomb potential between the final nuclei, in which case the first term of Eq. (2.2) is the Coulomb amplitude $-(2\pi\hbar^2/m)f_c(\theta)\delta_{fi}$, and $\chi_f^{(-)}$ is a Coulomb wave function. A partial-wave expansion of both $\chi_f^{(-)}$ and the incident Coulomb wave $\chi_i^{(+)}$ can be made. For example,

$$\chi_i^{(\pm)}=\sum_l i^l(2l+1)e^{\pm i\sigma_l}(kr_c)^{-1}F_l(kr)\times P_l(\cos\theta)|s\sigma\rangle|IK\rangle, \tag{2.3}$$

where σ_l is the Coulomb phase shift and $F_l(kr)$ the regular radial Coulomb wave function.

To evaluate the second term of Eq. (2.2), we divide configuration space into internal and external regions as described by Lane and Thomas,[8] and define surface functions at the various channel surfaces S_c.

$$|c)=\sum_{\sigma K\lambda\zeta}(l\lambda s\sigma|j\zeta)(j\zeta IK|JM)i^lY_{l\lambda}(\mathbf{r}_c)|s\sigma\rangle|IK\rangle. \tag{2.4}$$

These differ slightly from the surface functions defined in Ref. 8, first in the coupling scheme, and secondly in the lack of a factor $1/r$ in conformity with the work of Lane and Robson.[1]

We shall use the convention that a matrix element of the form $\langle\,|\,|\,\rangle$ implies integration over all coordinates, whereas elements of the form $(c|\,|\,\rangle$ or $(c|\,|c)$ imply integration only over the surface variables for the two separating nuclei, $dS_c=d\Omega_c d\xi_c$, where ξ_c are the internal variables and Ω_c the relative angular variables.

We make use of the surface operator[1,12]

$$\mathfrak{L}(b)=\sum_c|c)\frac{\hbar^2}{2m_c}\delta(r_c-a_c)\left(\frac{d}{dr_c}-\frac{b_c-1}{\alpha_c}\right)(c| \tag{2.5}$$

and denote by $\mathfrak{L}$ the operator corresponding to the particular case when b_c is set equal to L_c, the logarithmic derivative of an outgoing wave.[8] If H is the full Hamiltonian, and H_f the Hamiltonian corresponding to the Coulomb wave $\chi_f^{(-)}$, we may write

$$V_f-U_f=(H+\mathfrak{L}-E)-(H_f+\mathfrak{L}-E). \tag{2.6}$$

The Hermiticity of $(H_f+\mathfrak{L}-E)$ in the sense explained by Lane and Robson[1] and the relations

$$\mathfrak{L}\Psi_i^{(+)}=\mathfrak{L}\chi_i^{(+)},\quad \Psi_i^{(+)}=\mathcal{G}\mathfrak{L}\chi_i^{(+)} \tag{2.7}$$

may be used to obtain

$$\begin{aligned}\langle\chi_f^{(-)}|V_f-U_f|\Psi_i^{(+)}\rangle&=\langle\chi_f^{(-)}|\mathfrak{L}\Psi_i^{(+)}\rangle-\langle\mathfrak{L}^*\chi_f^{(-)}|\Psi_i^{(+)}\rangle\\&=\langle\chi_f^{(-)}|\mathfrak{L}\chi_i^{(+)}\rangle-\langle\mathfrak{L}^*\chi_f^{(-)}|\mathcal{G}|\mathfrak{L}\chi_i^{(+)}\rangle,\end{aligned} \tag{2.8}$$

where $\mathcal{G}=(H+\mathfrak{L}-E)^{-1}$ is a well-defined Green's operator.

We define the partial waves

$$\pi_c^{(\pm)}=2\left(\frac{\pm i}{\hbar v_c}\right)e^{\pm i\omega_c}\frac{1}{r_c}F_l(k_cr_c)|c). \tag{2.9}$$

The expansion [Eq. (2.3)] of $\chi_i^{(+)}$ and $\chi_f^{(-)}$ can be written in terms of these partial waves. Substituting the resulting expansions in Eq. (2.8), and choosing the

[10] M. Sano, S. Yoshida, and T. Teresawa, Nucl. Phys. 6, 20 (1958).

[11] C. C. Grosjean, Institut Interuniversitaire des Sciences Nucleaire, Monographie No. 7, Bruxelles (unpublished); A. Messiah, *Quantum Mechanics* (John Wiley & Sons, Inc., New York, 1966), Vol. II.

[12] C. Bloch, Nucl. Phys. 4, 503 (1954).

quantization axis along the beam direction, the amplitude T_{fi} becomes

$$T_{fi}=\frac{-2\pi\hbar^2}{(mm')^{1/2}}e^{2i\sigma_0}\frac{\pi^{1/2}}{k}\{-C(\theta)\delta_{fi}+i\sum_{ll'\lambda'jj'}\sum_{\xi\xi'JM}{}^{l}Y_{l'\lambda'}(\mathbf{k}')(l0s\sigma|j\xi)(j\xi IK|JM)\times(l'\lambda's'\sigma'|j'\xi')(j'\xi'I'K'|JM)T_{c'c}\}, \quad (2.10)$$

where

$$C(\theta)=\eta(4\pi)^{-1/2}\csc^2(\tfrac{1}{2}\theta)\exp\{-i\eta\ln[\sin^2(\tfrac{1}{2}\theta)]\},$$

and

$$T_{c'c}=\langle\pi_{c'}{}^{(-)}|\mathcal{L}\pi_c{}^{(+)}\rangle-\langle\mathcal{L}^*\pi_{c'}{}^{(-)}|\mathcal{G}|\mathcal{L}\pi_c{}^{(+)}\rangle. \quad (2.11)$$

The first term in Eq. (2.11) is the hard-sphere amplitude and is easily evaluated as

$$e^{2i\omega_c}(1-e^{-2i\varphi_c})\delta_{c'c},$$

where φ_c is the hard-sphere phase shift.[8] For the second term we note that

$$|\mathcal{L}\pi_c{}^{(+)}\rangle=(2i)^{1/2}P_c{}^{1/2}\Omega_c|\Phi_c\rangle, \quad (2.12)$$

where P_c is the penetrability, $\Omega_c=\exp\{i(\omega_c-\varphi_c)\}$, and

$$|\Phi_c\rangle=\left(\frac{\hbar^2}{2ma_c{}^3}\right)^{1/2}\delta(r_c-a_c)|c). \quad (2.13)$$

We introduce the set of R-matrix states $|\lambda\rangle$ which are solutions of the equation

$$[H+\mathcal{L}(b)-E_\lambda]|\lambda\rangle=0, \quad (2.14)$$

where b is a set of real boundary conditions. The Green's operator for these boundary conditions is

$$\mathcal{G}(b)=[H+\mathcal{L}(b)-E]^{-1}=\sum_\lambda\frac{|\lambda\rangle\langle\lambda|}{E_\lambda-E}. \quad (2.15)$$

The last expansion here is possible since $H+\mathcal{L}(b)$ commutes[1] with the summation $\sum_\lambda$. The relation between $\mathcal{G}(b)$ and $\mathcal{G}$ is

$$[1+\mathcal{G}(b)\Delta\mathcal{L}]\mathcal{G}=\mathcal{G}(b), \quad (2.16)$$

where

$$\Delta\mathcal{L}=\mathcal{L}-\mathcal{L}(b)=-\sum_c|\Phi_c\rangle L_c{}^0\langle\Phi_c|$$

and

$$L_c{}^0=L_c-b_c. \quad (2.17)$$

Thus we find that in matrix notation the amplitude $T_{c'c}$ becomes

$$\mathbf{T}=\mathbf{W}-\boldsymbol{\Omega}\{1+2i\mathbf{P}^{1/2}(1-\mathbf{RL}^0)^{-1}\mathbf{RP}^{1/2}\}\boldsymbol{\Omega}, \quad (2.18)$$

where

$$W_{cc'}=e^{2i\omega_c}\delta_{cc'},$$

$$R_{c'c}=\langle\Phi_{c'}|\mathcal{G}(b)|\Phi_c\rangle=\sum_\lambda\frac{\gamma_{\lambda c'}\gamma_{\lambda c}}{E_\lambda-E}, \quad (2.19)$$

and

$$\gamma_{\lambda c}=\langle\Phi_c|\lambda\rangle=\left(\frac{\hbar^2a_c}{2m_c}\right)^{1/2}(c|\lambda\rangle_{r_c=a_c}. \quad (2.20)$$

These last three equations, together with Eqs. (2.1) and (2.10) constitute the basic R-matrix formalism which we wish to use.

We turn now to the coupled-equation formalism. The full wave function is expanded in terms of the surface functions in Eq. (2.4):

$$\Psi_i{}^{(+)}=\sum_c\frac{1}{r_c}u_c(r_c)|c), \quad (2.21)$$

where the sum includes only channels of a fixed partition of the particles between target and projectile. Let H_I be the internal part of the Hamiltonian giving rise to the different target and projectile states occurring in $|c)$. Then

$$(H_I-\epsilon_c)|c)=0. \quad (2.22)$$

If T is the relative kinetic energy, the full Hamiltonian is

$$H=H_I+T+V_{\text{diag}}+V_{\text{coupl}}, \quad (2.23)$$

where the interaction has been split into a part which is diagonal in channel space, and a part which is not. Substitution of Eq. (2.21) into the Schrödinger equation leads to the coupled equations

$$[T_l+V_c(r)-(E-\epsilon_c)]u_c(r)=-\sum_{c'}V_{cc'}(r)u_{c'}(r), \quad (2.24)$$

where

$$T_l=\frac{-\hbar^2}{2m_c}\left[\frac{d^2}{dr^2}-\frac{l(l+1)}{r^2}\right],$$

$$V_c(r)=(c|V_{\text{diag}}|c),$$

$$V_{cc'}(r)=(c|V_{\text{coupl}}|c'). \quad (2.25)$$

Since the Hamiltonian is invariant under rotations and inversions, total angular momentum J and parity π are good quantum numbers and coupling occurs only between channels with the same values of (J,π). The problem is therefore to be solved for each value of (J,π) in turn.

We consider the case of nucleon scattering, and following Buck[6] we limit the target states to a 0^+ ground state and a 2^+ first excited state. For this case, at the most, six channels can contribute to a given value of (J,π).

For the diagonal part of the potential we use a real Saxon-Woods potential plus a spin-orbit term of the Thomas form:

$$V_c(r)=V_{\text{Coul}}(r)-V_sf_s(r)+2V_{\text{s.o.}}\left(\frac{\hbar}{m_\pi c}\right)^2r^{-1}\frac{\partial f_{\text{s.o.}}}{\partial r}\mathbf{l}\cdot\mathbf{s}, \quad (2.26)$$

where $V_{\text{Coul}}(r)$ is the Coulomb potential, $(\hbar/m_\pi c)^2$ has the value 2 F^2,

$$f_i(r)=\left[1+\exp\left\{\frac{(r-R_i)}{a_i}\right\}\right]^{-1}, \quad \text{and} \quad R_i=r_0{}^iA^{1/3}.$$

The suffix i represents either s or s.o. and A is the number of nucleons in the target. The nondiagonal part of the interaction is expressed in the form

$$V_{cc'}(r)=V_{II'}G_{cc'}g(r), \tag{2.27}$$

where

$$g(r)=-a_s\frac{\partial}{\partial r}f_s(r),$$

$$G_{cc'}=i^{l-l'}(-)^{J-1/2}\hat{j}\hat{j}'(j\tfrac{1}{2}j',-\tfrac{1}{2}|20)W(IjI'j';J2),$$

$$V_{02}=-\frac{\beta R_sV_s}{(4\pi)^{1/2}a_s}, \quad V_{22}=-\left(\frac{10}{7}\right)^{1/2}V_{02} \tag{2.28}$$

in the rotational model.[6]

The purpose of the work reported here is to solve these equations using R-matrix techniques, and to compare the results with the exact solutions obtained from the Buck coupled-equation program.

III. R-MATRIX SOLUTION OF COUPLED EQUATIONS

In applying R-matrix theory to coupled equations, we have to solve the coupled-equation eigenvalue problem corresponding to some real boundary conditions b at the surface separating internal and external regions. To help us do this we work with a basic set of states $|p\rangle$ corresponding to a model Hamiltonian H_0. The states $|p\rangle$ are then eigenstates of the equation

$$[H_0+\mathfrak{L}(b)-E_p']|p\rangle=0. \tag{3.1}$$

We take H_0 in this case to be that part of H which is diagonal in channel space:

$$H_0=H_I+T+V_{\text{diag}}, \tag{3.2}$$

so that the radial parts of $|p\rangle$ are eigenstates of the set of uncoupled equations

$$[T_l+V_c(r)-(E_p'-\epsilon_c)]v_{pc}(r_c)=0, \tag{3.3a}$$

satisfying the boundary conditions

$$a_c\left[\frac{d}{dr_c}v_{pc}(r_c)\right]_{r_c=a_c}=b_cv_{pc}(a_c). \tag{3.3b}$$

The states $|p\rangle$ clearly have zero components in all but one channel, so that each is a single-particle state in one or other of the channels,

$$|p\rangle=(1/r_c)v_{pc}(r_c)|c\rangle. \tag{3.4}$$

We can define uncoupled reduced-width amplitudes $\zeta_{pc}=(\hbar^2/2m_ca_c)^{1/2}v_{pc}(a_c)$ and for a given state $|p\rangle$, these are also zero in all but the one channel to which $|p\rangle$ belongs.

The R-matrix states

$$|\lambda\rangle=\sum_c\frac{1}{r_c}u_{\lambda c}(r_c)|c\rangle, \tag{3.5}$$

can be expressed in terms of this complete set

$$|\lambda\rangle=\sum_p M_{\lambda p}|p\rangle, \tag{3.6}$$

and similarly for the corresponding reduced width amplitudes $\gamma_{\lambda c}=(\hbar^2/2m_ca_c)^{1/2}u_{\lambda c}(a_c)$,

$$\gamma_{\lambda c}=\sum_p M_{\lambda p}\zeta_{pc}. \tag{3.7a}$$

This last equation may be written in matrix notation

$$\boldsymbol{\gamma}=\mathbf{M}\boldsymbol{\zeta}. \tag{3.7b}$$

Substituting Eq. (3.6) into Eq. (2.14) we obtain the matrix equation

$$\mathbf{M}(\boldsymbol{\mathcal{E}}'+\mathbf{V})=\boldsymbol{\mathcal{E}}\mathbf{M}, \tag{3.8}$$

where $\boldsymbol{\mathcal{E}}'$ and $\boldsymbol{\mathcal{E}}$ are diagonal matrices with elements E_p' and E_λ, respectively, and $\mathbf{V}$ has matrix elements

$$V_{p'p}=\langle p|V_{\text{coupl}}|p'\rangle=\int_0^\infty v_{pc}(r)V_{cc'}(r)v_{p'c'}(r)dr. \tag{3.9}$$

Here c and c' denote the channels to which $|p\rangle$ and $|p'\rangle$ belong.

The calculation to be performed then is first to solve the eigenvalue problem in Eq. (3.1) or Eq. (3.3) for the various levels in each channel, then form the matrix $\mathbf{V}$ from the integral in Eq. (3.9). Next we diagonalize the matrix $(\boldsymbol{\mathcal{E}}'+\mathbf{V})$ according to Eq. (3.8) to obtain the R-matrix levels E_λ and the transformation matrix $\mathbf{M}$. Reduced widths $\gamma_{\lambda c}{}^2$ can then be found from Eq. (3.7) and the R matrix formed. We then invert the 6×6 matrix $(\mathbf{1}-\mathbf{RL}^0)$ and calculate the amplitudes in Eqs. (2.18) and (2.10) and the cross section in Eq. (2.1).

Of course there is an infinite number of levels in each channel, and in practice we include only the nearby levels in our calculation, that is, those with energies near to the bombarding energies we wish to consider. The R matrix derived solely from these nearby levels[13] will be designated R^N:

$$R_{c'c}{}^N=\sum_{\lambda(\text{nearby})}\frac{\gamma_{\lambda c'}\gamma_{\lambda c}}{E_\lambda-E}, \tag{3.10}$$

and the method of calculation just described, where distant levels are completely ignored, is referred to

[13] The level energies and widths derived by diagonalizing only a limited number of states $|p\rangle$ are of course not exact either. Thus E_λ and $\gamma_{\lambda c}$ used in Eq. (3.10) are approximate values.

hereafter as method I. One of the attractive features of this technique is that the levels E_λ and widths $\gamma_{\lambda c}^2$ are energy-independent, so that once they have been determined, the amplitudes and cross sections for a finite range of energies are easily found.

It is desirable to include the effects of distant levels in some way, since it is known that they can combine together coherently and are an important factor in processes such as elastic scattering. The strength of these distant levels, however, lies in their numbers, more than anything else, so that it seems reasonable to suppose that they could be adequately represented by the uncoupled levels E_p and widths ζ_{pc}^2. We thus add a term

$$ {}^0R_{c'c}{}^D = \sum_{p(\text{distant})} \frac{\zeta_{pc'}\zeta_{pc}}{E_p'-E} \tag{3.11} $$

to the R matrix R^N as calculated in method I from nearby levels. An alternative way of viewing this process is to assume that there is zero coupling $V_{p'p}$ to and between these distant levels, so that the matrix $(\mathcal{E}'+\mathbf{V})$ in Eq. (3.8) is already diagonal in the distant levels. It is indeed reasonable that $V_{p'p}$ should be small for distant levels which oscillate rapidly as a function of r. We note that since ζ_{pc} is zero in all but one channel for fixed p, the distant-level contribution ${}^0R^D$ to the R matrix is diagonal in channel space. Despite this, the addition of this term affects the nondiagonal elements of the amplitude $T_{c'c}$ through the matrix inversion $(\mathbf{1}-\mathbf{RL}^0)^{-1}$.

In practice we cannot calculate ${}^0R_{cc}{}^D$ by summing over the infinite number of distant levels, but we make use of the fact that the uncoupled R function[8] in a given channel and for a given energy can be calculated exactly from the uncoupled wave function $v_c(E,r)$:

$$ {}^0R_{cc} = \left[\left\{ \frac{r}{v_c(E,r)} \frac{dv_c(E,r)}{dr} \right\}_{r_c=a_c} - b_c \right]^{-1}. \tag{3.12} $$

The wave function $v_c(E,r)$ is the regular solution of the equation

$$ [T_l + V_c(r) - (E-\epsilon_c)] v_c(E,r) = 0. \tag{3.13} $$

Thus if the contribution to ${}^0R$ from nearby levels is

$$ {}^0R_{cc}{}^N = \sum_{p(\text{nearby})} \frac{\zeta_{pc}{}^2}{E_p'-E}, \tag{3.14} $$

which we can calculate in practice, then ${}^0R_{cc}{}^D$ is easily obtained from

$$ {}^0R_{cc}{}^D = {}^0R_{cc} - {}^0R_{cc}{}^N. \tag{3.15} $$

According to this prescription therefore, the R matrix is calculated according to the formula

$$ \mathbf{R} = \mathbf{R}^N + {}^0\mathbf{R}^D, \tag{3.16} $$

and is used in the channel inversion $(\mathbf{1}-\mathbf{RL}^0)^{-1}$ to obtain amplitudes and cross sections. This method of including distant levels will be referred to as method II.

A third type of calculation has been tried which is not an R-matrix method. We express the channel amplitude $T_{c'c}$ in the form

$$ T_{c'c} = \langle \pi_{c'}{}^{(-)} | V | \Psi_c{}^{(+)} \rangle, \tag{3.17} $$

where V is the total interaction with Coulomb part subtracted out, and $\Psi_c{}^{(+)}$ is the solution of the full Schrödinger equation with the same incoming wave as $\pi_c{}^{(+)}$. This can be expanded into a distorted wave form similar to that used by Sano, Yoshida, and Teresawa,[10] as described by Lane and Robson.[1]

$$ \begin{aligned} T_{c'c} = {} & \langle \chi_{c'}{}^{(-)} | U^{\text{opt}} | \pi_c{}^{(+)} \rangle + \langle \chi_{c'}{}^{(-)} | (V-U^{\text{opt}}) | \chi_c{}^{(+)} \rangle \\ & - \langle \chi_{c'}{}^{(-)} | (V-U^{\text{opt}}) \mathcal{G} (V-U^{\text{opt}}) | \chi_c{}^{(+)} \rangle, \end{aligned} \tag{3.18} $$

where U^{opt} is some optical potential, and $\chi_c{}^{(+)}$ and $\chi_c{}^{(-)}$ are the corresponding distorted waves with incoming and outgoing parts the same as $\pi_c{}^{(+)}$ and $\pi_c{}^{(-)}$, respectively. To be more explicit, $\chi_c{}^{(+)}$ for example may be written

$$ \chi_c{}^{(+)} = 2\left(\frac{i}{hv_c}\right)^{1/2} e^{i(\omega_c+\delta_c)} f_c(r) | c \rangle, \tag{3.19} $$

where $f_c(r)$ is the regular solution of the radial Schrödinger equation with the optical potential U^{opt}, and δ_c is the complex nuclear phase shift.

The first term in Eq. (3.18) is simply the optical-model elastic-scattering amplitude:

$$ T_{c'c}{}^{\text{opt}} = e^{2i\omega_c}(1-e^{2i\delta_c})\delta_{c'c}. \tag{3.20} $$

The second term is the distorted-wave Born-approximation (DWBA) transition amplitude $T_{c'c}{}^{\text{DW}}$ and can be calculated in the usual way.

The third term carries all compound-nucleus effects. To evaluate it we introduce the complete set of model states $|p\rangle$ as before to get

$$ \begin{aligned} \sum_{pp'} & \langle \chi_{c'}{}^{(-)} | (V-U^{\text{opt}}) | p' \rangle \langle p' | \mathcal{G} | p \rangle \\ & \times \langle p | (V-U^{\text{opt}}) | \chi_c{}^{(+)} \rangle. \end{aligned} \tag{3.21} $$

The matrix elements

$$ \langle \chi_{c'}{}^{(-)} | (V-U^{\text{opt}}) | p' \rangle $$

and

$$ \langle p | (V-U^{\text{opt}}) | \chi_c{}^{(+)} \rangle $$

can be evaluated by direct numerical integration. The term $\langle p' | \mathcal{G} | p \rangle$ is an element of the level matrix $A_{p'p}$ defined by

$$ \begin{aligned} (A^{-1})_{p'p} &= \langle p' | (H+\mathcal{L}-E) | p \rangle \\ &= \langle p' | H_0 + \mathcal{L}(b) - E + h | p \rangle \\ &= (E_p'-E)\delta_{p'p} + V_{pp'} - \xi_{p'p}, \end{aligned} \tag{3.22} $$

where

$$ h = V_{\text{coupl}} + \mathcal{L} - \mathcal{L}(b). \tag{3.23} $$

$E_{p'}$ and $V_{p\bar{p}'}$ have already been defined in Eqs. (3.3)

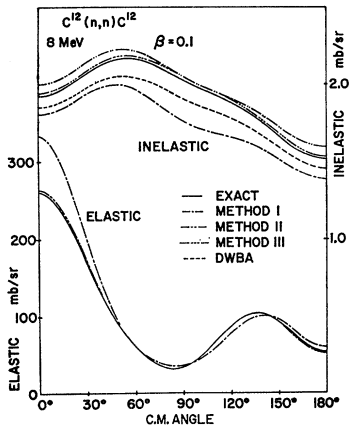

FIG. 1. Comparison of differential cross sections calculated by the three different methods for neutron scattering in a nonresonant region with weak coupling. Three levels per channel are included in the calculations, and the boundary conditions are $a_c=5.4$ F, $b_c=0$. The elastic curve for method III is not shown since it almost coincides with the curve for method II.

and (3.9), and from Eq. (2.17), we find

$$\xi_{p'p}=-\langle p|'\mathfrak{L}-\mathfrak{L}(b)|p\rangle=\sum_c \zeta_{p'c}L_c^0\zeta_{pc}. \quad (3.24)$$

The level matrix A may thus be evaluated by inversion of $(\mathcal{E}'-\mathbf{E}+\mathbf{V}^T-\xi)$ for nearby levels,[14] and the amplitude $T_{c'c}$ is then obtained. This method will be referred to as method III. The computation necessary for this method is somewhat longer as the potential matrix elements in Eq. (3.21) have to be calculated at every energy. In the calculations described in the next section, the real diagonal part of the potential in Eq. (2.26) was used instead of an optical potential for simplicity of programming, and the difference in potentials $V-U^{\text{opt}}$ occurring in Eq. (3.21) becomes merely the coupling potential V_{coupl}.

A computer program was written to perform these calculations. The uncoupled wave functions were checked by comparison with other programs performing similar calculations. The formation of the amplitude $T_{c'c}$ was checked from considerations of unitarity. From Eq. (2.18) we can show that for a real R matrix,

$$\sum_{c'\neq c}|T_{c'c}|^2=1-|(e^{2i\omega_c}-T_{cc})|^2. \quad (3.25)$$

This relation holds for the nearby level approximations for methods I and II but not for method III. The quantity (3.25) is called the transmission coefficient $T^{J\pi}$ if c is the entrance channel,[15] and by integration of the differential cross sections one can show that the total inelastic cross section is given by

$$\sigma_{\text{tot. inel.}}=\frac{\pi}{2k^2}\sum_{J,\pi}(2J+1)T^{J\pi}. \quad (3.26)$$

[14] The matrix $\mathbf{V}^T$ is the transpose of $\mathbf{V}$.

[15] There is only one entrance channel for a given (J,π) for a spin-zero target and spin-$\frac{1}{2}$ projectile.

A similar relation gives the total elastic cross section for neutron scattering:

$$\sigma_{\text{tot. el.}}=\frac{\pi}{2k^2}\sum_{J,\pi}(2J+1)|T_{cc}|^2, \quad (3.27)$$

where again c is the entrance channel. These total cross sections can also be calculated by numerical integration of the differential cross sections and this provides a check that the differential cross sections have been properly calculated.

The most convincing check of the program, however, is the good agreement obtained with the Buck coupled-equation program.

IV. CALCULATIONS

The calculations reported here were mainly done for a nucleon incident on a C^{12} target, which has a 2^+ first excited state at 4.433 MeV. The potential parameters used were as follows:

$$V_s=52\text{ MeV},\quad r_0{}^s=r_0{}^{s.o.}=1.267\text{ F},\quad (4.1)$$
$$V_{s.o.}=8\text{ MeV},\quad a_s=a_{s.o.}=0.400\text{ F}.$$

The Coulomb potential was assumed to be that for a uniform charge distribution over a sphere of radius R_s. Values of the deformation parameters used were $\beta=0.1$ for weak coupling or $\beta=\pm0.4$ for strong coupling. Since these parameters were chosen somewhat arbitrarily, the results are not expected to agree with experiment. In fact these variables are not to be considered as parameters in this work. They represent a fixed potential for which the exact elastic and inelastic scattering cross sections can be calculated using Buck's program. The aim of this work is to reproduce these cross sections using various R-matrix or level-matrix techniques, and the parameters available to us in this attempt are the R-matrix radii a_c, the boundary conditions b_c in Eq.

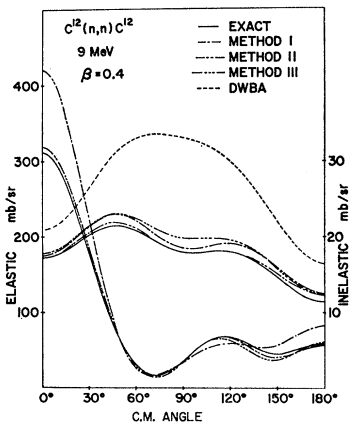

FIG. 2. Differential cross sections for neutron scattering with strong coupling. Three levels per channel are included in the calculations, and the boundary conditions are $a_c=5.4$ F, $b_c=0$.

(3.3b), and the number of nearby levels included in our calculations.

In general, the effect of varying a_c and b_c is very limited. The values of a_c and b_c were therefore fixed at $a_c=5.4$ F, $b_c=0$ for most of the following results. The policy with regard to the number of levels was to include all the levels within a certain energy range. For example, we find that for most channels, there are three uncoupled levels $|p\rangle$ between -15 and 80 MeV. Naturally for channels with high orbital angular momentum l, less than three levels are included in this range. However, the lower l channels make the more important contribution so that we refer to the inclusion of levels in this energy range as the "3 levels per channel" approximation. Since six channels contribute in general for a fixed value of (J,π), the diagonalization in this case involves up to 18 levels. In none of the figures shown have the results been scaled by an arbitrary factor to improve the fit.

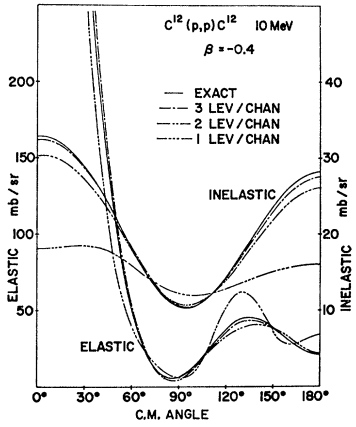

FIG. 4. Comparison of differential cross sections for proton scattering calculated by method II with varying numbers of levels per channel. The boundary conditions are $a_c=5.4$ F, $b_c=0$.

A. Nonresonant Region

Angular distributions for incident neutrons in a nonresonant energy region, are shown in Figs. 1 and 2, where the three methods described earlier, are compared. Method I gives good qualitative agreement, although a consistent error of this method is to overestimate the elastic forward peak. Presumably distant levels combine coherently to reduce this peak. The inclusion of distant levels by either of methods II or III gives excellent results. Method III is especially good for weak coupling (see Fig. 1), where the DWBA result [the first two terms of Eq. (3.18)] is quite good to start with. For stronger coupling (see Fig. 2) the DWBA result is too large as expected and method III not quite so good as method II.

In Fig. 3 some results for proton scattering with strong coupling are shown and again very good agreement is obtained.

Next we consider the effects of varying the number of levels. Since method II gives good results and is somewhat quicker than method III, we have used method II to compare the angular distributions obtained by including fewer levels. As seen in Fig. 4, good agreement is still obtained with only two levels per channel. The "one-level" case shown actually includes two levels for some of the negative-parity channels. One of these is a $1p_{3/2}$ or $1p_{1/2}$ level at about -5 MeV and the other is taken from a $2p_{3/2}$, $2p_{1/2}$, or $1f_{7/2}$ group at about 15 MeV. However, only one even-parity level is included, a $2s_{1/2}$, $1d_{5/2}$, or $1d_{3/2}$ level. The nearest excluded levels are the next even-parity levels at around 25 MeV. As we remarked earlier, these levels are approximately included in method II in the matrix ${}^0R^D$. However, as seen from Fig. 4, the agreement for the one-level case has deteriorated; presumably coupling of the levels at about 25 MeV via the coupling potential is of some importance in this strong-coupling case.

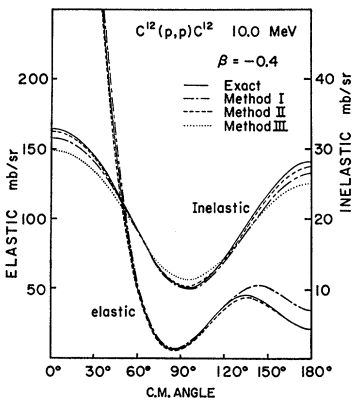

FIG. 3. Differential cross sections for proton scattering with strong coupling. Three levels per channel are included in the calculations, and the boundary conditions are $a_c=5.4$ F, $b_c=0$.

The effect of varying the parameters a_c and b_c for a nonresonant region is very small for methods II and III if 3 levels per channel are included. The results are good whatever boundary conditions are used. For method I, variation of the boundary conditions has more effect, but is not expected to be of value in getting better fits. An exact fit to the cross section at a given energy is possible even in the one-level approximation if we could use the boundary conditions satisfied by the physical wave function at that energy. But of course we cannot know these physical boundary conditions in advance. In general they can take any value and vary with energy. Similar considerations apply to methods II and III when fewer levels are included.

Figure 5 shows the angular distributions calculated by method II for protons scattered from Ti^{48}. Again the potential parameters were arbitrarily chosen. In this case four levels per channel were included to obtain this fit, since for this heavier nucleus the levels are closer together.

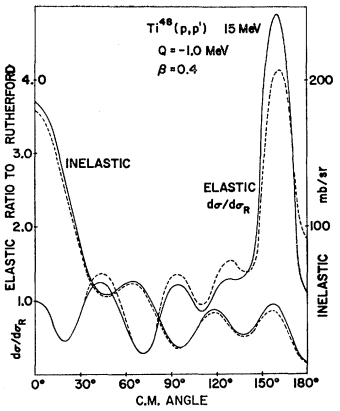

FIG. 5. Differential cross sections for proton scattering from a medium-weight nucleus calculated by method II. Four levels per channel were included in the diagonalization, and the boundary conditions are $a_c=7.2$ F, $b_c=0$.

B. Resonant Region

Channel coupling can lead to resonance phenomena[16] in the excitation function, and the potential parameters given at the beginning of this section for protons provide an example. Using the boundary conditions $a_c=5.4$ F and $b_c=0$, an uncoupled $d_{5/2}$ single-particle level arises in the inelastic channels at 5.54 MeV. (This energy includes the single-particle energy, plus 4.43-MeV excitation of the target.) This level can couple with the 2^+ core to give levels with spins $\frac{1}{2}+$, $\frac{3}{2}+$, $\frac{5}{2}+$, $\frac{7}{2}+$, and $\frac{9}{2}+$ in the compound system. With zero coupling, there is no way these levels can be formed (nor can they decay), so that they will not show up in elastic scattering, and inelastic scattering will be zero anyway. As we turn on channel coupling, the position of these compound levels alters so that they are no longer degenerate, and they show up as resonances in both the elastic and inelastic scattering. The $\frac{7}{2}+$ and $\frac{9}{2}+$ levels are still very weak due to the very small $l=4$ penetrability, and we shall consider only the $\frac{1}{2}+$, $\frac{3}{2}+$, and $\frac{5}{2}+$ resonances. An R-matrix treatment must be able to give the positions and widths of such resonances with reasonable accuracy.

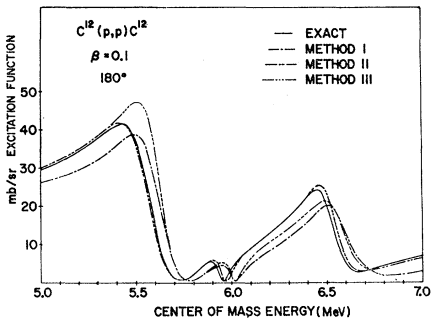

FIG. 6. Comparison of elastic excitation functions in a region of resonances calculated by the three methods. Three levels per channel are included and the boundary conditions are $a_c=5.4$ F, $b_c=0$.

[16] S. Okai and T. Tamura, Nucl. Phys. **31**, 185 (1962).

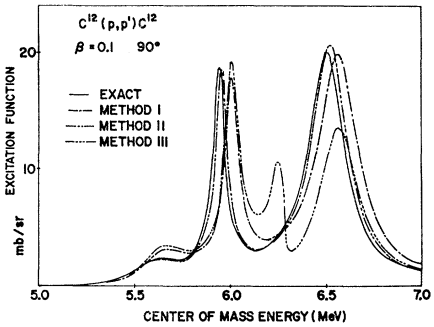

FIG. 7. Inelastic excitation functions in a region of resonances calculated by the three methods. Three levels per channel and boundary conditions $a_c=5.4$ F, $b_c=0$.

In Figs. 6 and 7 examples of the elastic and inelastic excitation functions are shown, and the three methods of calculation are compared, each including three levels per channel. In all cases good agreement is obtained for the elastic case, method II being the best. For the inelastic results, an interesting feature is the false peak at 6.25 MeV in the curve for method III. The DWBA excitation function for this region shows a single large resonance at 6.25 MeV, rising to over 100 mb/sr, representing a one-step transition to the single-particle level which is located at this energy.[17] The third term in Eq. (3.18) has to remove this resonance as well as provide the correct resonances, and as we see from Fig. 7, it is only partially successful in the attempt. Here again, method III would be improved by using optical distorted waves, in which case a far less pronounced DWBA resonance would arise.

For a more detailed investigation of these resonances it is convenient to use the transmission coefficients $T^{J\pi}$ defined by Eq. (3.25), which separate the different resonances. In view of the difficulty of the false resonance associated with method III we now confine our attention to methods I and II. Figure 8 shows the

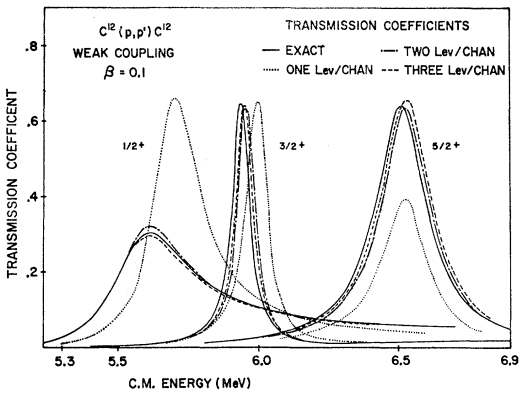

FIG. 8. Comparison of transmission coefficients calculated by method II with varying numbers of levels per channel. Boundary conditions $a_c=5.4$ F, $b_c=0$.

[17] The conversion to physical boundary conditions is responsible for the shift from 5.54 MeV mentioned earlier.

TABLE I. The composition of the $\frac{5}{2}^+$ R-matrix level in the two-level-per-channel approximation for the boundary conditions $a_c=5.4$ F, $b_c=0$.

s p level	Energy E_p (MeV)	Reduced widths ζ_{pc}	Coefficient $M_{\lambda p}$	$M_{\lambda p}^2$
2^+ $1d_{5/2}$	5.537	0.7672	0.9604	0.9224
2^+ $2s_{1/2}$	7.152	−1.2496	−0.2296	0.0527
0^+ $1d_{5/2}$	1.104	0.7672	0.1552	0.0241
0^+ $2d_{5/2}$	21.270	−1.6703	−0.0179	0.0003
2^+ $3s_{1/2}$	29.236	1.4744	−0.0151	0.0002
2^+ $1d_{3/2}$	13.327	1.2083	0.0127	0.0002
2^+ $2d_{5/2}$	25.703	−1.6703	−0.0061	0.0000
2^+ $1g_{9/2}$	29.756	1.5573	0.0053	0.0000
2^+ $1g_{7/2}$	34.383	1.8239	−0.0029	0.0000
2^+ $2d_{3/2}$	31.074	−1.4605	0.0026	0.0000

transmission coefficients calculated by method II for the three resonances, with varying numbers of levels. The result of including only two levels per channel seems in this case to be as good as including three levels per channel. A marked deterioration occurs however if only one level per channel is included. Let us consider the

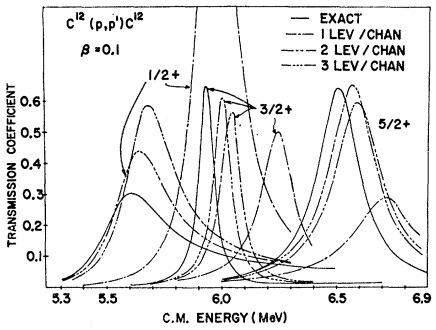

FIG. 9. Comparison of transmission coefficients calculated by method I with varying numbers of levels per channel. Boundary conditions $a_c=5.4$ F, $b_c=0$.

$\frac{5}{2}^+$ level as an example. Table I lists the various single-particle levels which contribute to the R-matrix level in the two-level approximation with boundary condition $b_c=0$. As stated earlier, the one-level approximation excludes coupling to the $2d_{5/2}$, $3s_{1/2}$, and $2d_{3/2}$ levels over 20 MeV. The $(0^+,2d_{5/2})$ single-particle state at 21.27 MeV has a reduced-width amplitude ζ_{pc} about twice[18] that of the $(0^+,1d_{5/2})$ state at 1.104 MeV. Thus the small $2d_{5/2}$ mixture increases the reduced-width amplitude $\gamma_{\lambda c}$ of the R matrix by about 25% in the entrance channel, and the partial width $\Gamma_{\lambda c}$ by about 50%; hence the much larger strength of the $\frac{5}{2}^+$ resonance in the two-level approximation.

[18] It is interesting to observe that single-particle widths, for boundary conditions $b_c=0$, are very small for negative energies, slowly increase as energy rises and reach a maximum perhaps exceeding the Wigner limit at 20 MeV or so, and then fall off to an average value for higher energies. This behavior can be understood by considering the shapes of the normalized wave functions at various energies.

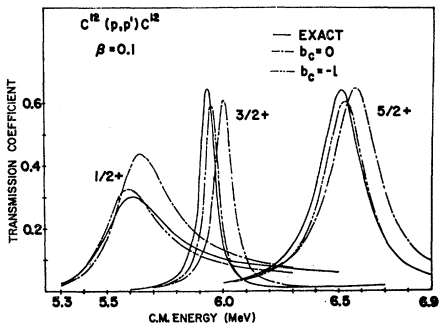

FIG. 10. Transmission coefficients calculated by method I with three levels per channel and different boundary conditions. R-matrix radius $a_c=5.4$ F, and the energy scale at the bottom is in MeV.

In Fig. 9 we consider the same resonances calculated by method I, using different numbers of levels per channel. We note that the results have deteriorated somewhat from those obtained by method II. The distant levels approximately included in method II can only affect the inelastic transmission coefficients through the surface matrix $\mathbf{L}^0$. Comparison of Figs. 8 and 9 thus indicates the effect of coupling to distant levels at the surface.

The obvious way to reduce this coupling is to minimize the matrix $\mathbf{L}^0$. The resonances we are considering are about an MeV or so above the inelastic threshold at 4.43 MeV. At these energies, the real part S_c of L_c is approximately given by $S_c=-l$ in the inelastic channels, while the imaginary part P_c, the penetrability, is already small. The matrix can be roughly minimized, therefore, by choosing the boundary conditions $b_c=-l$, sometimes referred to as "natural" boundary conditions. This choice is perhaps not so good in the elastic channel. Nevertheless, Fig. 10 shows that method I, using three levels per channel, can be improved near these resonances by using "natural" boundary conditions.

In method II a good fit is obtained anyway if we include three levels per channel, and variation of the boundary conditions has very little effect on the transmission coefficients. In fact the difference is so small that it is not worth including a diagram to show it. For

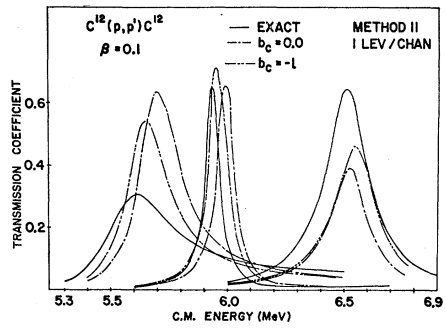

FIG. 11. Transmission coefficients calculated by method II with one level per channel and different boundary conditions. R-matrix radius $a_c=5.4$, and energy scale in MeV.

only one level per channel however, as we saw earlier, the fit is not as good because of coupling via the coupling potential to single-particle levels just above 20 MeV. Naturally, choice of boundary conditions cannot be expected to compensate for this effect and as indicated in Fig. 11, the choice $b_c=-l$ does not improve the fit significantly.

Let us consider now the underlying R-matrix levels. In order that we may use R-matrix calculations in a study of nuclear structure it is desirable that the R-matrix levels should provide a reasonably accurate description of the physical states. However, despite being able to fit the $\frac{5}{2}^+$ transmission coefficients with widely differing boundary conditions ($b_c=0$ as in Fig. 8, or $b_c=-l$), the structure of the corresponding R-matrix states is significantly different in the two cases, the $2S_{1/2}$ contribution being about 5% in the first case, and 20% in the second. This is perhaps to be expected since the boundary condition $b_c=0$ is not very physical. For an isolated resonance the R-matrix state probably does give a reasonably accurate description of the physical state, provided that the boundary conditions are chosen such that $b_c\approx S_c(E)$, where E is the energy of the resonance. This choice ensures that the R-matrix level energy E_λ lies within the resonance peak. If two or more resonances with the same spin and parity partially overlap one another however, the structure of the R-matrix states may change considerably even with small changes in the boundary conditions. This is not necessarily a criticism of R-matrix theory however, since the physical states themselves probably vary considerably with energy, and depend on the reaction used to form them.

We would also like to be able to obtain resonance parameters, for example the total widths, from the R-matrix levels. In the R-matrix one-level approximation, the total width is given by $\Gamma=2\sum_c P_c\gamma_{\lambda c}^2$. Taking the $\frac{5}{2}^+$ resonance as an example again, this formula leads to a value of about 0.75 MeV (using the boundary condition $b_c=-l$), which is about three times the resonance width as measured from Fig. 8. A similar effect occurs for the $\frac{3}{2}^+$ level. This narrowing of the widths is caused by interference with nearby levels of the same spin and parity. In particular there are two broad levels with spins $\frac{3}{2}^+$ and $\frac{5}{2}^+$ at about 7.5 MeV. These levels arise mainly from the $(2^+,2s_{1/2})$ single-particle level and are fairly weak in the entrance channel, so that they do not show up in either the elastic or inelastic scattering or the transmission coefficients. In order to explain this narrowing of the levels, we split the R matrix into two parts,[8] $\mathbf{R}_0$ and $\mathbf{R}_1$, corresponding to two sets of levels. Using the notation of a reduced-width matrix defined in connection with Eq. (3.7) one derives the relation[19]

$$(\mathbf{1}-\mathbf{R}\mathbf{L}^0)^{-1}\mathbf{R}=(\mathbf{1}-\mathbf{R}_0\mathbf{L}^0)^{-1}\mathbf{R}_0+\boldsymbol{\alpha}_1^T(\boldsymbol{\varepsilon}_1-\mathbf{E}-\boldsymbol{\xi}_1)^{-1}\boldsymbol{\alpha}_1, \quad (4.2)$$

where

$$\boldsymbol{\alpha}_1=\boldsymbol{\gamma}_1(\mathbf{1}-\mathbf{L}^0\mathbf{R}_0)^{-1}. \quad (4.3)$$

$\boldsymbol{\alpha}_1^T$ is the transpose of $\boldsymbol{\alpha}_1$, and

$$\boldsymbol{\xi}_1=\boldsymbol{\gamma}_1\mathbf{L}^0(\mathbf{1}-\mathbf{R}_0\mathbf{L}^0)^{-1}\boldsymbol{\gamma}_1^T. \quad (4.4)$$

The situation is especially clear if we consider only two levels, one at energy E_0 leading to R_0, and the other at E_1 leading to R_1. It is also convenient to choose boundary conditions $b_c=S_c(E_1)$, so that in the neighborhood of E_1, the single-level shifts $\Delta_{\lambda\lambda}=-\sum_c S_c^0\gamma_{\lambda c}^2$ are zero. Then the first term of Eq. (4.2) is a background term, while the second term determines the resonance parameters for the level at E_1, and becomes

$$\frac{\boldsymbol{\alpha}_1^T\boldsymbol{\alpha}_1}{E_1-E+\Delta_1-\frac{1}{2}i\Gamma_1}, \quad (4.5)$$

where

$$\Gamma_1=\Gamma_{11}-W_1,$$

$$\Delta_1=\frac{E_0-E_1}{\Gamma_{00}}W_1,$$

$$W_1=\frac{\Gamma_{00}\Gamma_{10}^2}{4(E_0-E_1)^2+\Gamma_{00}^2},$$

$$\Gamma_{\lambda\mu}=2\sum_c \gamma_{\lambda c}P_c\gamma_{\mu c}.$$

The observed width for this resonance is then Γ_1 which is less than the single-level width Γ_{11}, since W_1 is clearly positive. If the level at energy E_0 is fairly broad (say of the same order as the spacing E_0-E_1) this reduction can be quite large, and there is a shift Δ of the resonance towards E_0. An algebraically similar type of analysis to the above has been used in the discussion of giant resonance theory where a quantity similar to $-W_1$ is referred to as the spreading width.[20] The narrowing of resonances situated in the tails of neighboring levels has also been noted by Robson and Toutenhoofd.[21] Their treatment shows that the resonance width is reduced by a factor $\cos^2(\delta_c+\phi_c)$.

V. CONCLUSIONS

The calculations presented show that R-matrix methods can provide a practical means of calculation for the coupled-equation problem, and that adequate numerical accuracy is possible if enough levels are included.

Three methods have been described. In method I a set of uncoupled states is diagonalized to form the R-matrix states and distant levels are ignored. Good qualitative agreement with exact results is found.

[19] The second term here corresponds to the expression

$$\sum_{\lambda\mu}(\boldsymbol{\alpha}_\lambda\times\boldsymbol{\alpha}_\mu)A_{\lambda\mu}$$

in Ref. 8, where a direct product notation is used.

[20] D. Robson and A. M. Lane (to be published).

[21] D. Robson and W. Toutenhoofd, Australian J. Phys. 16, 370 (1963).

Better results are obtained if distant levels are approximately allowed for as in method II. In method III distant levels are accounted for by using distorted waves in the entrance and exit channels, and dealing with the compound system through a level matrix rather than an R matrix. Good agreement is again obtained except that false DWBA resonances tend to appear unless the distorted waves are generated by an absorptive potential.

As far as time of computation is concerned, the search for uncoupled eigenstates and diagonalization of the levels in methods I and II is the most time consuming part. This means that for calculation of angular distributions at a single energy, the methods described here take longer than a conventional coupled-equation calculation by about a factor of 5. However, it is normally desirable to fit angular distributions at more than one energy, and if several energies are needed, the two methods become equivalent as far as computation time is concerned, since the eigenvalue search and diagonalization need only be done once. For the calculation of excitation functions where 20 or more energies are needed, an R-matrix type of calculation becomes faster. In method III, the level-matrix inversion and calculation of potential matrix elements must be done at every energy, and method III is therefore usually somewhat longer.

It is usually necessary when fitting experimental data to do a parameter search, varying the potential parameters. Since the division of the interaction in Eq. (2.23) into a diagonal and a coupling part is to some extent arbitrary, it is possible when varying the parameters to keep the diagonal part fixed and vary only the coupling part. This would mean that the uncoupled eigenvalue search need only be done once, so that only the diagonalization would have to be repeated for different sets of parameters.

It is worth mentioning that methods I and II may also be done by a level-matrix technique. The Green's operator in Eq. (2.11) is evaluated as in method III in terms of the level matrix in Eq. (3.22). The numerical results of such a calculation are identical with those obtained by diagonalization and formation of the R matrix. The level-matrix methods take longer, however, if many energies are involved, and in addition, the approximate inclusion of distant levels is more natural and more convenient in the R-matrix approach. From a calculational viewpoint therefore, the R matrix is preferred to the level matrix, although this is at variance with the preference for the level matrix expressed recently by Mahaux.[22]

We note also that the R-matrix technique provides us with a set of concrete levels with definite energies and widths which are useful in explaining the structure of the compound system. For isolated resonances, the R-matrix level gives a good description of the physical state if boundary conditions are wisely chosen. When levels of the same spin and parity interfere with one another, the analysis of the situation is more difficult and R-matrix single-level parameters do not agree with the resonance parameters. Most theories of nuclear reactions have some difficulty in dealing with such a situation. As we have seen from our calculation, this difficulty in parametrizing the physical levels does not prevent us from calculating the excitation functions accurately over the corresponding resonances.

We have confined our attention solely to real potentials. This has the advantage that the uncoupled eigenvalues are real and makes the search for them easier. If it is desired to use complex optical potentials we must either search for complex eigenvalues, or absorb all of the complex parts into the coupling potential, so that V_{diag} is still Hermitian. In either case, we then have to diagonalize a non-Hermitian matrix which will lead to complex R-matrix energies. In this case, it may be preferable to revert to the level-matrix formulation mentioned two paragraphs back, since the level-matrix inversion is complex even for real potentials.

An alternative calculational technique can also be valuable in providing new theoretical modifications to the calculation. For example, antisymmetrization can be dealt with in the R-matrix approach by using antisymmetric R-matrix states. It is also possible to use various different nuclear models to describe the target nucleus.

ACKNOWLEDGMENTS

The author is grateful to Dr. D. Robson for suggesting this work, and for many valuable discussions. He is indebted to Mrs. Ellen Gille for helping with the programming, and to W. Thompson for providing some of the computer routines. Finally he would like to thank Dr. R. H. Davis and the Department of Physics for the hospitality extended to him while at Florida State University.

[22] C. Mahaux, Nucl. Phys. **79**, 481 (1966).